Dynamic Analysis of the KNTU CDRPM:
A Cable Driven Redundant Parallel Manipulator

Pooneh Gholami, Mohammad M. Aref and Hamid D. Taghirad†

***Abstract*— KNTU CDRPM is a cable driven redundant parallel manipulator, which is under investigation for possible high speed application such as 3D laser cutting machine. This newly developed mechanisms have several advantages compared to the conventional parable mechanisms. Its rotational motion range is relatively large, its redundancy improves safety for failure in cables, and its design is suitable for high acceleration motions. In this paper, the inverse kinematic analysis of this structure in is presented first, and then the Jacobian matrices of the manipulator are derived. Furthermore, the governing dynamic equation of motion of such structure is derived using the Newton-Euler formulation. Next, the dynamic equations of the system is used in simulations. It is shown that on the contrary to serial manipulators, dynamic equations of motion of parallel manipulators can be only represented implicitly, and only special integration routines can be used for their simulations. In order to verify the accuracy and integrity of the derived dynamics, open– and closed–loop simulations for the system is performed and analyzed. It is shown that high gain PD controllers are able to reduce the induced vibration caused by the cable structures in these manipulators.**

I. Introduction

Increasing performance requirements necessitates design of new types of manipulators with larger dexterous workspace with higher accelerations. Parallel manipulators can generally perform better than serial manipulators in terms of stringent stiffness and acceleration requirements. In parallel manipulators, each actuated leg has to carry only a part of the payload; this is quite energy efficient and the robot can handle heavy load to weight ratios. On the other hand, it also implies that the end-effector moves slower than the actuated joints. However, limited workspace and existence of many singular regions inside the workspace of the parallel manipulators limits the applications of parallel manipulators. Moreover, mechanical elements such as spherical joints make it difficult to manufacture such mechanisms at a low cost [1]. In the cable driven redundant parallel manipulators (CDRPM), the hydraulic linear actuators of parallel manipulators are replaced with electrical powered cable drivers which leads immediately to a wider workspace. As an example consider the Sky-Cam, which is a cable driven robotic camera that covers wide area of a Football stadium [2], [3]. Higher acceleration of the moving platform imposed at longer times frames, can be reached by CDRPM as a result of using light moving parts, such as the one used in the WARP virtual acceleration robot [4]. Having over–constrained low mass moving platform, ultra–high speed with more than 40g can be attained by this manipulator [5].

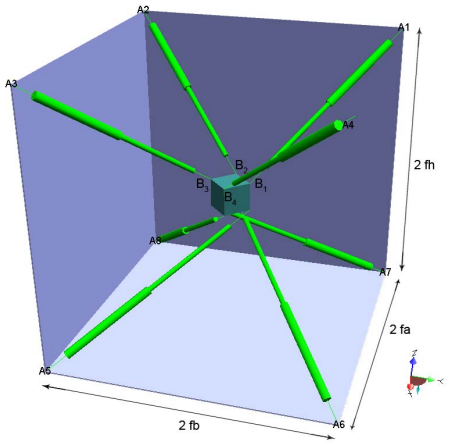

Fig. 1. The KNTU CDRPM, a Perspective View

The payoffs of these large advantages of CDRPM is some challenging topics of research in the robotics community. A CDRPM has complicated forward kinematics [6], cables are sagged under compression forces, and redundancy resolution is a necessity in these type of robots. NIST RoboCrane design have tried to solve these problems with an under–constrained moving platform that suspended from the roof with the gravity force. This approach is useful only for low accelerated heavy moving platform applications such as shipping crane, or a such platform for serial manipulators [7]. To achieve tension forces on cables in a dextrous workspace, moving platform have to become over–constrained [8]. In this paper, such specific structure which is called as CDRPM for brevity. KNTU CDRPM refers to the manipulator under investigation which is designed in the K.N. Toosi University of Technology for 3D Laser cutting applications. KNTU CDRPM uses a novel design to achieve stiffness, precision and high-speed moving platform.

In this paper the dynamic analysis of this parallel manipulator is studied in detail. Such analysis is an essential step to design such manipulators in a way to accomplish the required task, within its entire workspace. In this analysis the inverse kinematics and Jacobian matrices of the manipulator is derived first. The traditional Newton–Euler formulation is used for the dynamic analysis of general parallel manipulators [9], and also for the Stewart platform, which is the most celebrated parallel manipulator [10]. In this formulation all

the reaction forces can be computed, which is very insightful for the design of CDRPM. On the other hand, the equations of motion for each limb and the moving platform must be derived, which inevitably leads to a large number of equations. It is shown that on the contrary to serial manipulators, dynamic equations of motion of such parallel manipulators can be only represented implicitly. Therefore, special integration routines are used for the simulations and verifications. Among the many control topologies reported in the literature, the dynamics and control of redundantly actuated parallel manipulators has been considered by fewer researchers [11]. In order to verify the accuracy and integrity of the derived dynamics, open– and closed–loop simulations for the system is performed and analyzed. It is shown that a decentralized PD controllers are able to reduce the induced vibration caused by the cable structures in these manipulators.

II. Kinematics

A. Mechanism Description

The KNTU Cable Driven Redundant Parallel Manipulator is illustrated in figure 1. This figure shows a spatial six degrees of freedom manipulator with two degrees of redundancy. This robot has eight identical cable limbs. The cable driven limbs are modeled as spherical-prismatic-spherical(SPS) joints because cables can only bear tension force neither radius nor bending force. The moving platform is illustrated as a cubic box in here for simplicity, However, in the analysis it is considered to have arbitrarily chosen attachment points, in order to simulate the end-effector of a 3D laser cutting machine. For the purpose of analysis, two cartesian coordinate systems $A(x, y, z)$ and $B(u, v, w)$ are attached to the fixed base and moving platform. Points $A_1, A_2, \cdots, A_8$ lie on the fixed cubic frame and $B_1, B_2, \cdots, B_8$ lie on the moving platform. The origin O of the fixed coordinate system is located at the centroid of the cubic fixed frame. Similarly, the origin G of the moving coordinate system is located at centroid of the cubic moving platform. The transformation from the moving platform to the fixed base can be described by a position vector $\overrightarrow{g} = \overrightarrow{OG}$ and a 3×3 rotation matrix ${}^{A}R_{B}$. Consider a_i and ${}^{B}b_i$ be the position vectors of points A_i and B_i in the coordinate system A and B, respectively. Although in the analysis of the KNTU CDRPM, all the attachment points, can be arbitrarily chosen, the geometric and inertial parameters given in table I is used in the simulations.

B. Inverse Kinematics

Similar to other parallel manipulator, CDRPM has complicated forward kinematics [6], and inverse kinematic is used for dynamic modeling. Therefore, in this section, the kinematic of the system is studied in detail. As illustrated in figure 1,the B_i points lie at the vertexes of the cube. For inverse kinematic analysis of the cable driven parallel manipulator, it is assumed that the position and orientation of the moving platform $x = [x_G, y_G, z_G]^T$, ${}^{A}R_{B}$ is given and the problem is to find the joint variable of the CDRPM, $\boldsymbol{L} = [L_1, L_2, \ldots, L_8]^T$. From the geometry of the manipulator as illustrated in figure 2, the loop closure equation for each limb, $i = 1, 2, \ldots, 8$, can be written as,

$$ {}^{A}\overrightarrow{A_iB_i} + {}^{A}\overrightarrow{a_i} = {}^{A}\overrightarrow{g} + {}^{A}\boldsymbol{T}_{B}({}^{B}\overrightarrow{b_i}) \tag{1} $$

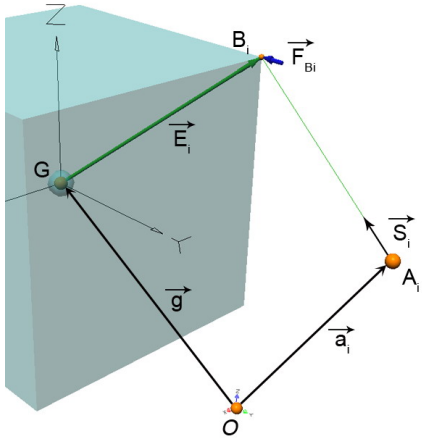

Fig. 2. ith Attachment Point on the Moving Platform and Related Vectors

in which, ${}^{A}\boldsymbol{T}_{B}$ is the homogeneous transformation matrix corresponding to the moving frame B with respect to the fixed frame A. The length of the i'th limb is obtained through taking the dot product of the vector $\overrightarrow{A_iB_i}$ with itself. Therefore, for $i = 1, 2, \ldots, 8$

$$ L_i^2 = [{}^{A}\boldsymbol{g} + {}^{A}\boldsymbol{T}_{B}({}^{B}\boldsymbol{b}_i) - {}^{A}\boldsymbol{a}_i]^T [{}^{A}\boldsymbol{g} + {}^{A}\boldsymbol{T}_{B}({}^{B}\boldsymbol{b}_i) - {}^{A}\boldsymbol{a}_i] \tag{2} $$

As shown in figure 2

$$ L_i = \left\{ [\boldsymbol{g} + \boldsymbol{E}_i - \boldsymbol{a}_i]^T [\boldsymbol{g} + \boldsymbol{E}_i - \boldsymbol{a}_i] \right\}^{\frac{1}{2}} \tag{3} $$

If the solution of L_i becomes a complex number, then the location of the moving platform is not reachable.

C. Jacobian

Jacobian analysis plays a vital role in the study of robotic manipulators [14]. Let the actuated joint variable be denoted by a vector $\boldsymbol{L}$ and the location of the moving platform be described by a vector $\boldsymbol{x}$. Then the kinematic constrains imposed by the limbs can be written in the general form $\boldsymbol{f}(\boldsymbol{x}, \boldsymbol{L}) = 0$ by differentiating with respect to time, we obtain a relationship between the input joint rates and the end-effector output velocity as follows :

$$ J_x \dot{\boldsymbol{x}} = J_L \dot{\boldsymbol{L}} \tag{4} $$

where $J_{\boldsymbol{x}} = \frac{\partial \boldsymbol{f}}{\partial \boldsymbol{x}}$ and $J_{\boldsymbol{L}} = -\frac{\partial \boldsymbol{f}}{\partial \boldsymbol{L}}$. The derivation above leads to two separate Jacobian matrices Hence the overall Jacobian matrix J can be written as:

$$ \dot{\boldsymbol{L}} = \boldsymbol{J} \cdot \dot{\boldsymbol{x}} \tag{5} $$

where $\boldsymbol{J} = \boldsymbol{J}_L^{-1} \boldsymbol{J}_{\boldsymbol{x}}$. Jacobian matrix not only reveals the relation between the joint velocities $\dot{\boldsymbol{L}}$ and the moving platform

TABLE I
Geometric and Inertial Parameters of the KNTU CDRPM

Description	Quantity
f_a: Half of the length of the fixed cube	$1\ m$
f_b: Half of the width of the fixed cube	$1.5\ m$
f_h: Half of the height of the fixed cube	$2\ m$
C : Half of dimension of the cubic moving platform	$0.1\ m$
M: The moving platform's mass	$5\ Kg$
I: The moving platform's moment of inertia	$0.033\ Kg \cdot m^2$
ρ: The limb density per length	$0.007\ Kg/m$
K_p: The gain of proportional	100
K_d: The gain of derivative	10

velocities $\dot{\boldsymbol{x}}$, but also constructs the transformation needed to find the actuator forces $\boldsymbol{\tau}$ from the forces acting on the moving platform $\boldsymbol{F}$. When J_L is singular and the null space of J_L is not empty, there exist some nonzero $\dot{\boldsymbol{L}}$ vectors that result zero $\dot{\boldsymbol{x}}$ vectors which called serial type singularity and when J_x becomes singular, there will be a non-zero twist $\dot{\boldsymbol{x}}$ for which the active joint velocities are zero. This singularity is called parallel type singularity [15]. In this section we investigate the Jacobian of the CDRPM platform shown in figure 1. For this manipulator, the input vector is given by $\boldsymbol{L} = [L_1, L_2, \ldots, L_8]^T$, and the output vector can be described by the velocity of the centroid G and the angular velocity of the moving platform as follows :

$$\dot{\boldsymbol{x}} = \begin{bmatrix} \boldsymbol{V}_G \\ \boldsymbol{\omega}_G \end{bmatrix} \tag{6}$$

Jacobian matrix of a parallel manipulator is defined as the transformation matrix that converts the moving platform velocities to the joint variable velocities, as shown in equation 5. Therefore, the CDRPM Jacobian matrix J is a non-square 8×6 matrix. The Jacobian matrix can be derived by formulating a velocity loop-closure equation for each limb. Referring to figure 2, a loop-closure equation for the ith limb is written in equation 1. In order to obtain the Jacobian matrix, let us differentiate the vector loop equation 1 with respect to time, considering the vector definitions $\hat{S}_i$ and $\overrightarrow{E_i}$ illustrated in figure 2. Hence, for $i = 1, 2, \cdots, 8$:

$$\boldsymbol{V_G} + \boldsymbol{\omega}_G \times \boldsymbol{E_i} = \dot{L}_i \hat{\boldsymbol{S}}_i + L_i \left(\boldsymbol{\omega}_i \times \hat{\boldsymbol{S}}_i\right) \tag{7}$$

Furthermore $\boldsymbol{\omega}_i$ denotes the angular velocity of i'th limb with respect to the fixed frame A. To eliminate $\boldsymbol{\omega}_i$, dot-multiply both sides of equation 7 by S_i.

$$\dot{L}_i = \hat{\boldsymbol{S}}_i \boldsymbol{V}_G + \left(\boldsymbol{E}_i \times \hat{\boldsymbol{S}}_i\right) \boldsymbol{\omega}_G \tag{8}$$

Rewriting equation 8 in a matrix form:

$$\dot{L}_i = \begin{bmatrix} \boldsymbol{S}_i \mid \boldsymbol{E}_i \times \hat{\boldsymbol{S}}_i \end{bmatrix} \cdot \begin{bmatrix} \boldsymbol{V}_G \\ \boldsymbol{\omega}_G \end{bmatrix} \tag{9}$$

Using equation 9 for $i = 1, 2, \ldots, 8$ the CDRPM Jacobian matrix J is derived as following.

$$\boldsymbol{J} = \left[\begin{array}{c|c} \hat{\boldsymbol{S}}_1^T & (\boldsymbol{E}_1 \times \hat{\boldsymbol{S}}_1)^T \\ \hat{\boldsymbol{S}}_2^T & (\boldsymbol{E}_2 \times \hat{\boldsymbol{S}}_2)^T \\ \vdots & \vdots \\ \hat{\boldsymbol{S}}_8^T & (\boldsymbol{E}_8 \times \hat{\boldsymbol{S}}_8)^T \end{array}\right] \tag{10}$$

Note that the CDRPM Jacobian matrix $\boldsymbol{J}$ is a non-square 8×6 matrix, since the manipulator is a redundant manipulator. To eliminate L_i, cross multiply both sides of equation 7 by $\hat{S}_i$:

$$\begin{aligned} L_i \boldsymbol{\omega}_i &= \hat{\boldsymbol{S}}_i \times \boldsymbol{V}_G + \hat{\boldsymbol{S}}_i \times \boldsymbol{\omega}_G \times \boldsymbol{E}_i \\ \boldsymbol{\omega}_i &= \frac{1}{L_i} \cdot (\hat{\boldsymbol{S}}_i \times \boldsymbol{V}_G + \hat{\boldsymbol{S}}_i \times \boldsymbol{\omega}_G \times \boldsymbol{E}_i) \end{aligned} \tag{11}$$

Therefore, $\boldsymbol{J}_\omega$ defined as the matrix relating the vector of moving platform velocities, $\dot{\boldsymbol{x}}$ to the vector of the limbs' passive joints angular velocities as:

$$\dot{\boldsymbol{\omega}}_i = \boldsymbol{J}_{\omega_i} \cdot \dot{\boldsymbol{x}} \tag{12}$$

in which, for $i = 1, 2, \ldots, 8$,

$$\boldsymbol{J}_{\omega_i} = \frac{1}{L_i} \left[\begin{array}{c|c|c|c|c|c} 0 & -S_{iz} & S_{iy} & E_{ix}S_{ix} & E_{ix}S_{iy} & E_{ix}S_{iz} \\ S_{iz} & 0 & S_{ix} & E_{iy}S_{ix} & E_{iy}S_{iy} & E_{iy}S_{iz} \\ -S_{iy} & S_{iz} & 0 & E_{iz}S_{ix} & E_{iz}S_{iy} & E_{iz}S_{iz} \end{array}\right] \tag{13}$$

When J_{ω_i} becomes singular, there exists a non-zero $\dot{\boldsymbol{x}}$ that results zero $\dot{\omega}_i$.

D. Accelerations

Acceleration analysis of the limbs and the moving platform is needed for Newton–Euler formulation. In this section, the acceleration analysis for the CDRPM manipulator is performed. Let us compute the linear and angular velocities of each limb in terms of the velocity and angular velocity of moving platform. The velocity of a point B_i, denoted as $\boldsymbol{V}_{bi}$, is found by taking the time derivative of the right-hand side of equation 1:

$$\boldsymbol{V}_{bi} = \boldsymbol{V}_G + \boldsymbol{\omega}_G \times \boldsymbol{E}_i \tag{14}$$

Transforming $\boldsymbol{V}_{bi}$ to the i'th limb frame yields ${}^i\boldsymbol{V}_{bi} = {}^iT_A \boldsymbol{V}_{bi}$. The velocity of B_i can also be written in terms of the angular velocity of the i'th limb by taking the derivative of the left-hand side of equation 1 with respect to time. We obtain the angular velocity of limb i :

$${}^i\boldsymbol{\omega}_i = \frac{1}{L_i} ({}^i\boldsymbol{S}_i \times {}^i\boldsymbol{V}_{bi}) \tag{15}$$

The acceleration of the ball point B_i, expressed in the fixed frame, is found by taking the time derivative of equation 14:

$$\dot{\boldsymbol{V}}_{bi} = \dot{\boldsymbol{V}}_G + \dot{\boldsymbol{\omega}}_G \times \boldsymbol{E}_i + \boldsymbol{\omega}_G \times (\boldsymbol{\omega}_G \times \boldsymbol{E}_i) \tag{16}$$

Expressing $\dot{\boldsymbol{V}}_{bi}$ in the i'th limb frame gives ${}^i\dot{\boldsymbol{V}}_{bi} = {}^i(T_A)\dot{\boldsymbol{V}}_{bi}$. The acceleration of B_i can be expressed in terms of the angular acceleration of the ith limb:

$${}^i\dot{\boldsymbol{V}}_{bi} = \ddot{L}_i\, {}^i\boldsymbol{S}_i + L_i\, {}^i\dot{\boldsymbol{\omega}}_i \times {}^i\boldsymbol{S}_i + L_i\, {}^i\boldsymbol{\omega}_i \times ({}^i\boldsymbol{\omega}_i \times {}^i\boldsymbol{S}_i) + 2\dot{L}_i\, {}^i\boldsymbol{\omega}_i \times {}^i\boldsymbol{S}_i \tag{17}$$

Dot-multiplying both sides of equation 17 by ${}^i\boldsymbol{S}_i$, we obtain

$$\ddot{L}_i = {}^i\dot{v}_{bi_z} + L_i\, {}^i\boldsymbol{\omega}_i^2 \tag{18}$$

in which, ${}^i\dot{v}_{bi_z}$ is the z component of the limb acceleration vector ${}^i\dot{\boldsymbol{V}}_{bi}$. Cross multiplying both sides of equation 17 by ${}^iS_i$, we obtain the angular acceleration of limb i:

$${}^i\dot{\boldsymbol{\omega}}_i = \frac{1}{L_i}\, {}^i\boldsymbol{S}_i \times {}^i\dot{\boldsymbol{V}}_{bi} - \frac{2\dot{L}_i}{L_i}\, {}^i\boldsymbol{\omega}_i \tag{19}$$

The required acceleration components for the dynamic analysis of CDRPM is fully derived.

III. Dynamic Analysis

A. Dynamic Modeling

The main approach of dynamic analysis of CDRPM is Newton-Euler method. In this approach the free-body diagrams of the components are considered separately. The Newton-Euler equations are applied to all limbs and moving platform containing external, contact and inertia forces or torques.

It is assumed that the moving platform center of mass is located at the geometrical center point G and it has a mass of M and moment of inertia I_G. Furthermore, since the manipulator is cable-driven, the mass of the limbs depend on

cable length. It is also assumed that the cables have circular cross section, and a constant density per unit length of ρ.

$$m = \rho L_i \tag{20}$$

Thus, the cables' moments of inertia are varying, and can be calculated assuming that they are circle section slender bars with varying length. As illustrated in figure 3, the moment of inertia of the cables around the fixed point A_i is given by:

$$I_{\text{Ai}} = \frac{1}{3}\rho L_i \begin{bmatrix} 0 & 0 & 0 \\ 0 & 1 & 0 \\ 0 & 0 & 1 \end{bmatrix} \tag{21}$$

Center of mass velocity vector for each limb contains two rotational and linear elements:

$$\boldsymbol{v}_{\text{ci}} = \frac{1}{2}(\dot{L}_i\hat{S}_i + L_i\omega_i \times \hat{S}_i) \tag{22}$$

$\hat{\boldsymbol{S}}_i$ is the unit vector along i'th cable, and the other unit vectors of cable's rotative coordinate are $\hat{\boldsymbol{N}}_i$ and $\hat{\boldsymbol{R}}_i$. They can be any unit vectors that make an orthogonal coordinate on the Ai fixed point. Thus, $\hat{\boldsymbol{N}}_i$ and $\hat{\boldsymbol{R}}_i$ are defined as:

$$\hat{\boldsymbol{N}}_i = \frac{\hat{\boldsymbol{S}}_i \times \boldsymbol{E}_i}{\|\hat{\boldsymbol{S}}_i \times \boldsymbol{E}_i\|} \tag{23}$$

$$\hat{\boldsymbol{R}}_i = \hat{\boldsymbol{S}}_i \times \hat{\boldsymbol{N}}_i \tag{24}$$

The Newton-Euler equations for varying mass cable can be written as:

$$\sum \boldsymbol{F}_{\text{ext}} = \frac{\partial}{\partial t}(m_i \boldsymbol{v}_{\text{ci}}) \tag{25}$$

$$\sum \boldsymbol{M}_{\text{Ai}} = \frac{\partial}{\partial t}(I_{\text{Ai}}\boldsymbol{\omega}_i) \tag{26}$$

According to acceleration of rotative velocity vector [16]. equations 25, 26 derived to:

$$\boldsymbol{F}_{\text{Bi}} - \boldsymbol{F}_{\text{Ai}} = \frac{1}{2}\rho L_i^2[\dot{L}_i\boldsymbol{\omega}_i \times \hat{\boldsymbol{S}}_i + \dot{\boldsymbol{\omega}}_i \times \boldsymbol{S}_i + \omega_i \times (\boldsymbol{\omega}_i \times \hat{\boldsymbol{S}}_i)] \tag{27}$$

$$\boldsymbol{F}^N_{\text{Bi}} + \boldsymbol{F}^R_{\text{Ai}} = \frac{1}{L_i}(\dot{I}_{\text{Ai}}\boldsymbol{\omega}_i + I_{\text{Ai}}\dot{\boldsymbol{\omega}}_i) \tag{28}$$

By using light weight cables such as the ones used in this manipulator, the gravity force effects on the cables can be ignored compared to the dynamic induced forces [17]. As shown in figure 3, F^S_{Ai} the cable's tension force applied by cable driver unit can be represented by:

$$\boldsymbol{F}^S_{\text{Ai}} = -\boldsymbol{\tau}_{\text{Ai}} \tag{29}$$

Relations between actuator forces and the end-effector affected forces had been studied in cable-affected forces. Writing the Newton-Euler equations for moving platform, describes the relation between forces, torques and acceleration of moving platform as following:

$$M\ddot{\boldsymbol{x}} = \boldsymbol{F}_D + M[0,\, 0,\, -9.81]^T + \sum_{i=1}^{n} \boldsymbol{F}_{\text{Bi}} \tag{30}$$

$$I_G\ddot{\boldsymbol{\theta}} = \boldsymbol{\tau}_D - \sum_{i=1}^{n} \boldsymbol{E}_i \times \boldsymbol{F}_{\text{Bi}} \tag{31}$$

In which, M and I_G are moving platform's mass and moment of inertia and n is number of the cables. F_D and $\boldsymbol{\tau}_D$ are

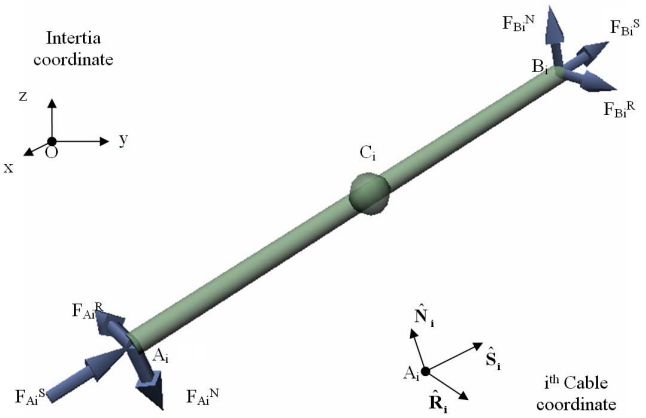

Fig. 3. ith Cable's rotative coordinate and force elements

disturbance forces and torques effects on moving platform with respect to fixed frame coordinate. Therefore, equations 30 and 31 can be viewed in two implicit 3×1 vector differential equations of the form:

$$\boldsymbol{f}_f(\boldsymbol{x}, \dot{\boldsymbol{x}}, \ddot{\boldsymbol{x}}, \boldsymbol{F}_D, \boldsymbol{\tau}) = 0 \tag{32}$$

$$\boldsymbol{f}_{tau}(\boldsymbol{\theta}, \dot{\boldsymbol{\theta}}, \ddot{\boldsymbol{\theta}}, \boldsymbol{\tau}_D, \boldsymbol{\tau}) = 0 \tag{33}$$

The use of these equation is two fold. The first use of it is to evaluate the actuator forces τ needed to produce a prescribed trajectory $\boldsymbol{x}(t)$ in presence of the disturbance forces and moments $\boldsymbol{F}_D, \boldsymbol{\tau}_D$. However, the governing equations of motion of the manipulator can be implemented for dynamic simulation of the system. For dynamic simulation, it is assumed that the actuator forces $\boldsymbol{\tau}(t)$, are given and the manipulator motion trajectory $\boldsymbol{x}(t)$, is needed to be determined.

B. Dynamical Validation

As explained before, the most important application of the dynamic equations of the CDRPM is the direct dynamic simulation of the system. In this case it is assumed that the actuator forces, are given and the manipulator motion is to be determined. Due to implicit nature of the dynamic equation, usual numerical integration routines such as Runge–Kutta methods [13], cannot be used to solve the problem. However, special integration routine[1], which is capable to integrate implicit functions, can be used for dynamic simulations. The first simulations is performed to verify the dynamic equations in order to have a trusted model. Thus, the model is tested in some scenarios in which the behavior of the system can be predicted by intuition.Free falling test of the moving platform results in an accelerated motion in -z direction. The free fall is slower than a free falling of the cubic body in the same condition which is reveals the effect of the cable inertia terms in the motion. In order to study the cable constrained motion of the moving platform, all tension forces of cables $\boldsymbol{\tau}_{Ai}$ are set to $100N$. In order to describe the simulated behavior of the system it is simpler to consider only the front view of CDRPM as shown in figure 4. In this scenario, the initial geometry of the moving platform is symmetric with respect to the x, y, and z axes, and all actuator forces acting on the moving platform have the same size. Therefore, the forces and

[1] `ode15i` function of Matlab

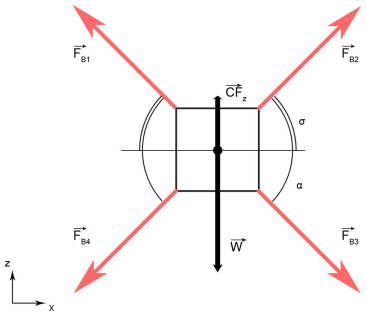

Fig. 4. Applied actuator forces: the vector sum is zero

torques are balanced statically and the resultant force acting on moving platform is zero. The simulation results confirms the static balance of the manipulator in this case. Nevertheless, when any other disturbance or displacement is applied, statical equilibrium is disturbed, and as illustrated in figure 5, in which $\vec{W}$ is the gravity force effect on the moving platform, has changed the force balance. In this case, the resultant force is in the z direction and the resulting motion is shown in figure 5. In order to study the motion of the moving platform in z direction, let us nominate CF_z as the resulting actuator forces in z direction:

$$\boldsymbol{CF_z} = \sum_{\boldsymbol{i=1}}^{\boldsymbol{8}} \boldsymbol{F}_{\mathrm{Bi}}^{\boldsymbol{z}} \tag{34}$$

As shown in figure 4, the resultant of the actuator forces $\boldsymbol{F}_{Bi}$ is in z direction and its magnitude can be given by:

$$CF_z = 2\sum_{i=1}^{4} {}^{B}F_{\mathrm{Bi}}^{S}(\mathrm{Sin}(\sigma) - \mathrm{Sin}(\alpha)) \tag{35}$$

Where σ angle is measured counter clockwise and α is measured clockwise. Using the manipulator geometry it can be shown that the sinusoid of the angles σ and α are a function of only the z variable as following:

$$\mathrm{Sin}(\sigma) = \frac{f_{fix} - z}{\mathrm{Li}} \tag{36}$$

$$\mathrm{Sin}(\alpha) = \frac{f_{fix} + z}{\mathrm{Li}} \tag{37}$$

since, F_{Bi}^{S} forces have same magnitudes while accelerations are small. Substituting equations 36, and 37 in equation 35,

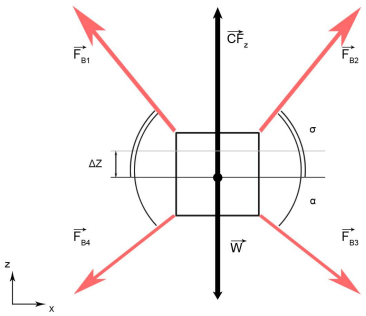

Fig. 5. Applied same actuator forces: the sum is nonzero

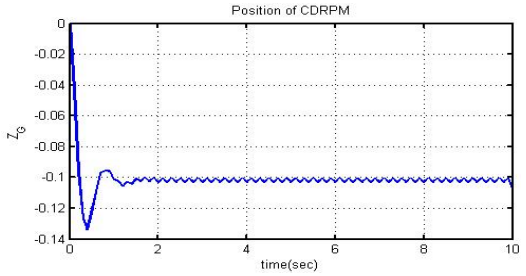

Fig. 6. Response of open–loop excitation by constant gravity force

the Newton-Euler equations in z direction can be simplified as the following differential equation:

$$M\ddot{z} = CF_z - W \tag{38}$$

collecting all fixed coefficients, and replacing them with two constant parameter K_o, and K_1. simplifies the dynamic equation into:

$$M\ddot{z} = k_o - k_1 z \tag{39}$$

Thus, the system behavior becomes similar to a free vibration in z direction without damping. As shown in figure 6, the simulation results of the dynamical model is also a free vibration in z direction, similar to the expected behavior. Similar scenarios are simulated in order to verify the dynamic behavior of the system, and in all cases similar correspondences are observed. Hence, the dynamic equation is used to analyze the closed loop performance of the system.

IV. Closed–Loop Performance

In order to analyze the closed–loop performance of the manipulator in hand a position control topology is simulates. Let's assume that the desired trajectory of the manipulator is given, and the actuator forces required to generate the trajectory must be generated. Notice that the governing equation of motion of the manipulators are six implicit differential equations given in equations 32 and 33. However, due to the actuator redundancy in the manipulator the number of unknown variables are eight. Therefore, there are infinitely many solutions for the eight actuator forces to solve the dynamic equations. Let us denote the resulting cartesian force/moments applied to the manipulator moving platforms $\mathcal{F}$. In this definition $\mathcal{F}$ is calculated from the summation of all inertial, and external forces *excluding the actuator torques* $\boldsymbol{\tau}$ in the dynamic equations 32 and 33. Due to the projection property of the Jacobian matrix [14], $\mathcal{F} = \boldsymbol{J}^T\boldsymbol{\tau}$ is the projection of the actuator forces on the moving platform, and can be uniquely determined from the dynamic equations by excluding the actuator forces from the dynamic equations. If the manipulator has no redundancy in actuation, the Jacobian matrix, $\boldsymbol{J}$, was squared and the actuator forces can be uniquely determined by $\boldsymbol{\tau} = \boldsymbol{J}^{-T}\mathcal{F}$, provided that $\boldsymbol{J}$ is nonsingular. For redundant manipulators, however, there are infinity many solution for $\boldsymbol{\tau}$ to be projected into $\mathcal{F}$. The simplest solution

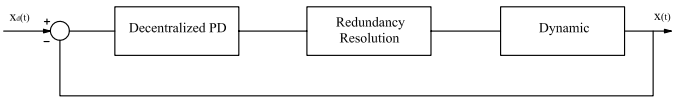

Fig. 7. Block Diagram of Closed-Loop

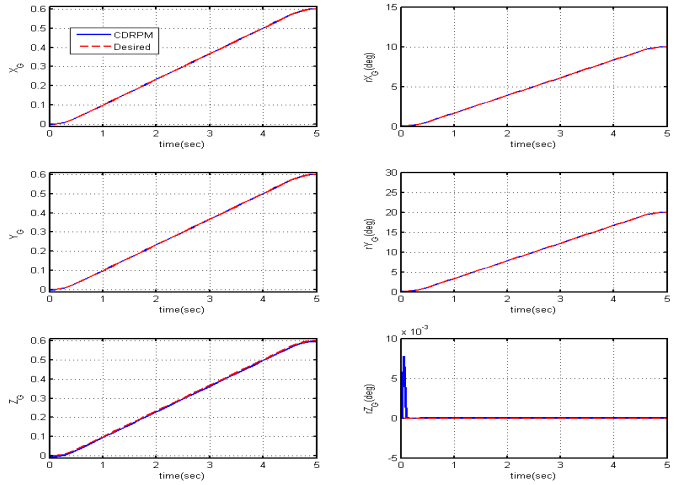

Fig. 8. Closed–Loop Performance

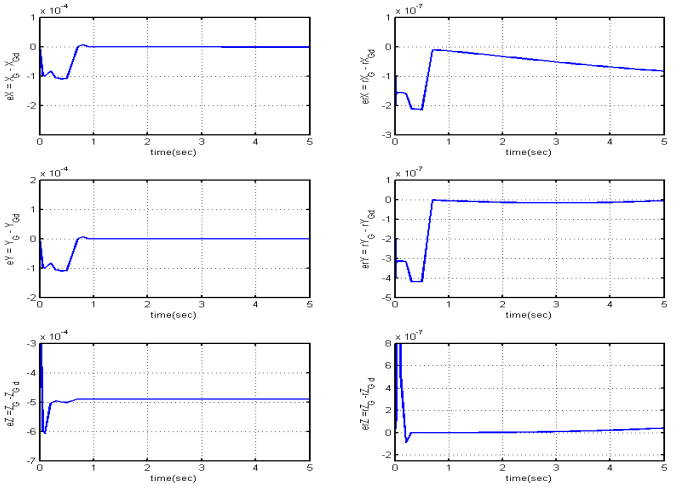

Fig. 9. Error of Position and Orientation in closed–loop

would be a minimum norm solution, which is found from the pseudo–inverse of $\boldsymbol{J}^T$, by $\boldsymbol{\tau} = \boldsymbol{J}^{T^\dagger}\mathcal{F}$. This solution is implemented in the simulation studies reported in this paper. Other optimization techniques can be used to find the actuator forces projected from $\boldsymbol{F}$ which can minimize a user defined cost function. The Block diagram of dynamic simulation in closed–form is given in figure 7. As shown in figure 7, pseudo–inverse of the main Jacobian, $J^{T^\dagger}$, is used as the redundancy resolution method. The controller used in this simulation is a decentralized PD controller, in which the gains are tuned such that the required tracking performance is achieved. The gains are given in table I. A linear trajectory with parabolic blends is considered in these simulation. The closed–loop tracking performance of the CDRPM is illustrated in figures 8 and 9. As seen in figure 9, a decentralized PD controller for CDRPM is capable of reducing the tracking errors less than $0.1mm$ in position and less than 0.05^o in orientation. The redundancy resolution technique used, however, is very simple, and can be further investigated to guarantee that the cables are in tension in all configuration of CDRPM maneuvers.

V. Conclusions

In this paper the dynamic analysis of KNTU CDRPM is studied in detail. This manipulator is a cable driven redundant parallel manipulator, which is under investigation for possible high speed application such as 3D laser cutting machine. Dynamic analysis is an essential step to design such manipulators in a way to accomplish the required performance, within its entire workspace. In this analysis the inverse kinematics and Jacobian matrices of the manipulator is derived first. The equation of motion of the manipulator is derived using Newton–Euler formulation. In this formulation all the reaction forces can be computed, which is very insightful for the design of CDRPM. It is shown that on the contrary to serial manipulators, dynamic equations of motion of such parallel manipulators can be only represented implicitly. Therefore, special integration routines are used for the simulations and verifications. In order to verify the integrity and the accuracy of the dynamic equations a simulation study is performed on the system for the open– and closed–loop scenarios. The integrity of the models are verified through the open–loop simulations, while It is shown that a decentralized PD controllers are able to reduce the induced vibration caused by the cable structures in these manipulators. It is shown that the obtainable tracking performance is less $0.1mm$ in position and less than 0.05^o in orientation.

References

[1] M. Hiller, Sh. Fang, S. Mielczarek, R. Vehoeven and D. Franitza. Design, analysis and realization of tendon-based parallel manipulators. *Mechanism and Machine Theory*, 40(2005) 429-445.

[2] K. Usher, G. Winstanley, P. Corke and D. Stauffucher. Air Vehicle Simulator: An Application for a Cable Array Robot. In *IEEE Conf. Robotics and Automution*, pages 2241–2246, April. 2005.

[3] L. L. Cone. Skycam: an aerial robotic camera system, Byte, pp.122-132, Oct. 1985.

[4] S. Tadokoro and T. Matsushima. A Parallel Cable-Driven Motion Base for Virtual Acceleration. *IEEE Int. Conf. Intelligent Robots and Systems*, pages 1700–1705, Nov. 2001.

[5] S. Kawamura, H. Kino, and Ch. Won. High-Speed Manipulation by Using Parallel Wire-Driven Robots. *Robotica*, pages 13-21, 2000.

[6] S. Song and D. Kwon. Geometric Formulation Approach for Determining the Actual Solution of the Forward Kinematices of 6-DOF Parallel Manipulators. In *IEEE Int. Conf. Intelligent Robots and Systems*, pages 1930–1935, Oct. 2002.

[7] S. E. Landsberger and T.B. Sheridan, A New Design for Parallel Link Munipulator. In *Proc Systems, Man and Cybernetics*, pages 8-12, 1985.

[8] C.B. Pham, S.H. Yeo, G. Yang, M.Sh. Kurbanhusen and I.M. Chen. Force-Closure Workspace Analysis of Cable-Driven Parallel Mechanisms . *Mechanism and Machine Theory*, 41(2006) 53-69.

[9] C.Gosselin. Parallel computational algorithms for the kinematics and dynamics of planar and spatial parallel manipulators . *Trans. ASME Journal of Dynamic Systems, Measurement and Control*, 118(1):22-28,1996.

[10] N. Dasgupta and T.S. Mruthyunjaya A Newton-Euler formulation for the inverse dynamics of the stewart platform manipulator. *Mechanism and Machine Theory*, 33(8):115-52, 1998.

[11] Hui Cheng and Yiu-Kuen Yiu and Zexiang Li. Dynamics and control of redundantly actuated parallel manipulators. *IEEE/ASME Transactions on Mechatronics*, 8(4):483-491, Dec. 2003.

[12] J.P. Merlet. Still a Long Way to Go to the Road for Parallel Manipulator . *ASME 2002 DETC Confrance*, Montral, Canada, 2002.

[13] L. F. Shampine, *Numerical solution of ordinary differential equations*, Chapman & Hall, New York, 1994.

[14] L.W. Tsai. Robot Analysis. *John Wiley and Sons ,Inc*, pages 223-228, 1999.

[15] J.P. Merlet. Parallel Robots. *Spring*, page 180, 2006.

[16] R.C. Hibbler. Engineering Mechanics: Dynamics. *Prentice Hall College Div*, January, 1995.

[17] Xiumin Diao and Ou Ma. Workspace Analysis of a 6-DOF Cable Robot for Hardware-in-the-Loop Dynamic Simulation. *IEEE/RSJ Int.Conf. IROS 2006*, 2006.